

# 1 **Limitations in the Landsat satellite archive bias SDG monitoring**

2 Ruben Remelgado<sup>1,2\*</sup>, Christopher Conrad<sup>1,3</sup>, Carsten Meyer<sup>2,3,4\*</sup>

## 3 **Affiliations:**

- 4 1. German Centre for Integrative Biodiversity Research (iDiv), Halle-Leipzig-Jena, Leipzig, Germany  
5 2. Chair of Computational Landscape Ecology, Technical University of Dresden, Dresden, Germany  
6 3. Institute of Geosciences and Geography, Martin Luther University Halle-Wittenberg, Halle (Saale), Germany.  
7 4. Institute of Biology, Leipzig University, Leipzig, Germany  
8 \*co-corresponding authors

## 9 **Highlights**

- 10 1) Coverage and quality of historical Landsat satellite data are spatiotemporally uneven  
11 2) Global time-series of forest, arable-land and water inherit signals of these limitations  
12 3) The limitations cause bias in perceived land changes with sustainability implications  
13 4) Biased change perceptions are more likely in lower-income countries  
14 5) Developers and users of remote-sensing data both have a part in minimising biases

## 15 **ABSTRACT**

16 Satellite remote sensing is vital for monitoring, research, and policy addressing  
17 sustainability challenges from climate and ecosystem changes to food and water security. Here,  
18 Landsat satellite data play a crucial role, thanks to their unique global, long-term, and high-  
19 resolution coverage. Yet, gaps and quality limitations in the Landsat data archive may  
20 propagate into derived remote-sensing products and thereby threaten the validity of  
21 downstream applications, especially when data users have limited training in remote sensing.  
22 To improve awareness of these issues, we here demonstrate that global, historical Landsat data  
23 are spatially and temporally uneven, frequently interrupted, and have seasonally incomplete  
24 coverage and quality. Using a causal-discovery framework, we moreover show that these  
25 limitations are inherited in several state-of-the-art, global time-series products, biasing  
26 perceptions of changes in forests, arable-lands, and water resources. These biases can impair  
27 reliable assessments of environmental and human development issues targeted by the  
28 Sustainable Development Goals (SDG) framework, and disproportionately affect lower-  
29 income countries. We provide global data-quality information to support the explicit  
30 consideration of potential biasing effects in future uses of remote-sensing products derived  
31 from Landsat data, and discuss avenues towards better uncertainty reporting and bias control  
32 in satellite-based sustainability monitoring and related applications.

33

34 **Keywords:** remote sensing, sustainability, post-2020, Landsat, SDG

## 35 **1. INTRODUCTION**

36 193 countries committed to 17 Sustainable Development Goals (SDGs, UN general  
37 Assembly, 2015) to comprehensively address the environmental and social impacts of  
38 economic development. Yet, nearing the target year 2030, we are still far from meeting these  
39 goals (Moyer and Hedden, 2020). Widespread and rapid land alterations (Winkler et al., 2021)  
40 cause biodiversity loss (IPBES, 2019), accelerate climate change and threaten regional food

41 and water security (UN DESA, 2022). The global 2030 SDG Agenda foresees regular progress  
42 monitoring and reporting as a basis for their periodic recalibration (Xu et al., 2020), and to  
43 identify national responsibilities for sustainability issues that help secure practical  
44 commitments (Perino et al., 2022).

45 Satellite remote sensing allows monitoring many SDG indicators at multiple spatial and  
46 temporal scales (Anderson et al., 2017) and, thanks to open-data policies of key satellite  
47 archives (Wulder and Coops, 2014), (geo)computational advances (Cracknell, 2018), and  
48 investments in technical capacity-building (Mora and Wijaya, 2012), has become a primary  
49 tool for countries to meet their reporting obligations (Anderson et al., 2017, p. 20).

50 In particular, the Landsat program (Zhu et al., 2019) fulfils a vital role for continuous land-  
51 surface monitoring due to its unique combination of long historical coverage (**Fig. 1a**) and  
52 relatively high spatial and temporal image resolution (30-m since 1982, typically every 16-  
53 days). Thanks to the program's longevity, Landsat data are key to evaluating long-term  
54 environmental changes against historical baselines (ESA, 2020), or in response to human  
55 interventions (Schmidt-Traub et al., 2017). Moreover, Landsat data support forward-looking  
56 policy support by enabling credible future scenario projections to anticipate emerging  
57 development issues and calibrate political action (Gregory et al., 2012). Correspondingly,  
58 Landsat data have become an integral part of a growing number of mapping applications  
59 supporting SDG monitoring (e.g., Pekel et al., 2016; Potapov et al., 2022; Vancutsem et al.,  
60 2021). Yet, the Landsat archive has extensive gaps due to historical data losses (Wulder et al.,  
61 2016, **Fig. 1b**), and available data face quality issues due to, for instance, cloud cover (Ju and  
62 Roy, 2008) or data degradation (Wulder et al., 2016).

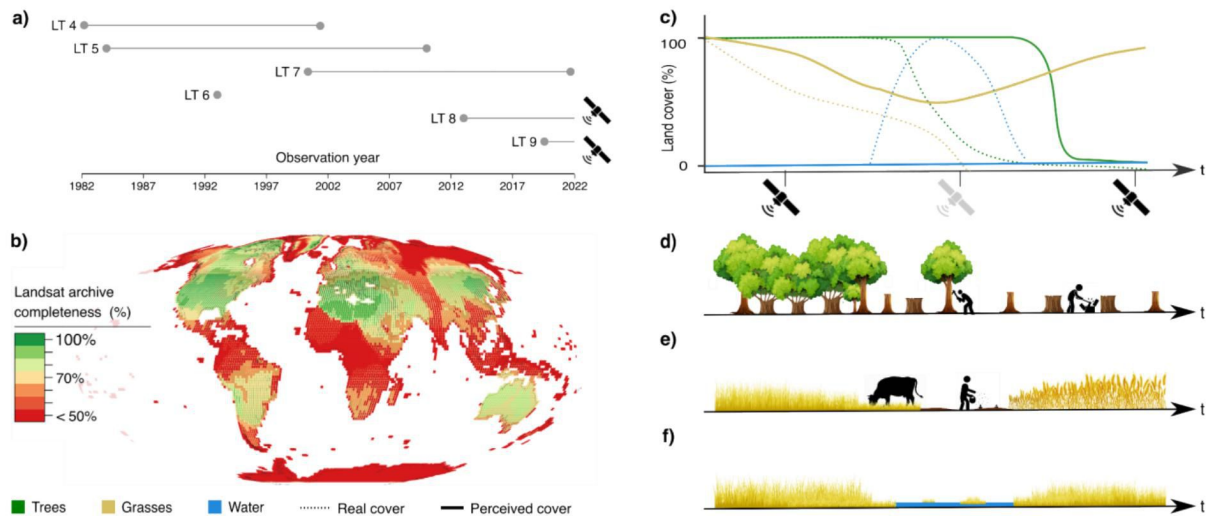
63 Remote sensing experts are generally aware of such issues. In fact, remote sensing literature  
64 discusses how data volumes and intra-annual temporal coverages affect the robustness of  
65 spectral metrics (Frantz et al., 2023) that ultimately inform remote sensing products, and how  
66 stringent quality controls impact data volumes (Zhang et al., 2022). Furthermore, extensive  
67 literature provides technical recommendations on how to tackle inconsistent data coverages.  
68 This includes seasonal and epoch-based compositing (Hansen et al., 2013; Potapov et al.,  
69 2022), filling of data gaps by harmonising multiple sensors (Claverie et al., 2018), or detecting  
70 changes continuously to tackle interruptions in data coverage (Vancutsem et al., 2021; Zhu and  
71 Woodcock, 2014). Many resulting products are then validated using strict protocols (e.g.,  
72 through sample-based assessments of accuracy, area, and uncertainty, Olofsson et al., 2014).

73 However, although existing literature and protocols address various limitations in satellite  
74 data, they cannot completely prevent their propagation into derived data products. In fact, many  
75 applications remain sensitive to satellite data availability. For instance, they may respond  
76 negatively to the lack of observations over specific dates (e.g., when monitoring deforestation,  
77 Sales et al., 2022, or land uses, Fan et al., 2022; Prishchepov et al., 2012), or require  
78 observations spread consistently throughout a year (e.g., when mapping phenology, Mas and  
79 Soares de Araújo, 2021, e.g., to monitor vegetation responses to climate change, Ma et al.,  
80 2022). Moreover, remote sensing data products ultimately reach broad user communities that  
81 include resource managers, policy-makers, and scientists of different disciplines, many of  
82 whom have limited or no training in remote sensing. These communities are unlikely to engage  
83 with the existing, mostly technical literature on data limitations that is targeted at remote

84 sensing experts. In fact, a recent survey suggests that users are largely unfamiliar with the  
 85 limitations of Landsat-based data products (Molder et al., 2022).

86 To improve the use of remote sensing data products in downstream applications, there is a  
 87 need for studies that sensitise users and non-expert developers about their inescapable  
 88 uncertainties. This will ultimately improve the transparency of science communication,  
 89 limiting the risk of data misuses, and combating distrust in scientific data caused by  
 90 misunderstandings of uncertainties (Gustafson and Rice, 2020). Here, we take needed steps to  
 91 bridge between data users and producers.

92 First, we demonstrate the magnitude of spatial and temporal variations of data limitations in  
 93 the global, historical Landsat archive since the launch of the first 30-metre-resolution sensor in  
 94 1982, which paved the way to a multitude of scientific advances in satellite remote sensing. To  
 95 this end, we map the between- and within-year frequency, recurrence, and quality of daytime  
 96 Landsat images. Second, we use a causal inference framework to demonstrate how spatial and  
 97 temporal variations in these dimensions of quality affect our perception of changes in the extent  
 98 of forests (**Fig. 1d**), arable lands (**Fig. 1e**), and seasonal surface water (**Fig. 1f**) mapped by  
 99 state-of-the-art products relevant for SDG monitoring. Third, we evaluate whether data-  
 100 quality-related biases in perceptions of change vary across countries with differing financial  
 101 capabilities to sustain sophisticated national monitoring systems. Finally, we provide  
 102 recommendations on how to improve the reporting of data limitations, and how to best include  
 103 them in future remote sensing data products.



104 **Figure 1. Temporal gaps in satellite observations and their conceptual link to biased perceptions of land changes.** a)  
 105 Five operational Landsat (LT) satellite missions provided a seemingly uninterrupted global coverage for 1982-2022 (grey  
 106 lines; satellite icons indicate active missions). b) However, the Landsat archive provides much less continuous data. c) Data  
 107 gaps influence our perception of change trajectories. Dashed lines depict true trajectories, and continuous lines show  
 108 trajectories measured with satellite data. In the x-axis, satellite observations (black satellite icons) are temporarily interrupted  
 109 (grey satellite icon). During the observation period, the y-axis measures changes in percentages of trees (in green, d), grasses  
 110 (in yellow, e-f), and surface water (in blue, f). Note no solid water line is shown due the absence of satellite data. d) Data gaps  
 111 hide the start of logging, leading new satellite observations to perceive abrupt changes. e) Grassland losses due to grazing  
 112 precede the planting of wheat, but data gaps during this transition makes these indistinguishable leads us to perceive grassland  
 113 losses followed by grassland gains. f) Similarly to d), data gaps hide temporal variation in the proportions of (savanna) grasses  
 114 that are seasonally covered by water.  
 115

116 **2. METHODS**117 **2.1. Quantification of satellite data limitations**

118 We developed a suite of metrics on the annual and year-to-year frequency and recurrence  
119 of Landsat images, weighted by their respective quality. The quality of individual images  
120 directly reflects geometric and spectral issues (USGS, 1998) and cloud cover (Ju and Roy,  
121 2008), and indirectly shadows and haze, which typically accompany clouds. We calculated our  
122 metrics for each year, and for each descending tile drawn in the World Reference System 2  
123 (USGS, 1998). We then combined tile-level metrics by averaging them into global 1-km-  
124 resolution grid cells, while taking into account tile overlaps. We obtained the data feeding our  
125 metrics from the metadata provided with each Landsat acquisition (USGS, 2021). We used all  
126 metadata recorded between 1982 and 2022, but disregarded those relating to Landsat's  
127 Multispectral Scanner System imagery, which are not commonly used in remote sensing  
128 applications due to their lower spatial and spectral resolution compared to Landsat 4-9.

129 **Image quality.** We created a normalised metric between 0 (worst) and 1 (best) on the quality  
130 of each Landsat image  $j$  (QI). For a given year  $y$  and tile  $t$ , QI is given by  $Q_{y,t,i} / 9 * (100 - C_{y,t,i})$ ,  
131 where  $C$  is the cloud-cover percentage at the time of the image acquisition.  $Q$  is a qualitative  
132 metric between 0 and 9 that is used by the United States Geological Survey to grade the number  
133 of bad scans in an image (USGS, 1998).

134 **Within-year variations in data quality.** In each year, we used the estimated QI of each  
135 corresponding satellite image – but excluding those with QI=0, which implies the absence of  
136 any usable data – to calculate several within-year quality metrics. First, we summed the QI of  
137 all images, weighing annual image frequencies by the proportion of usable pixels (hereafter  
138 'quality-weighted frequency'). Second, we counted the number of months with images to  
139 measure our ability to perceive within-year (e.g., seasonal) changes. Third, we estimated the  
140 maximum QI as a proxy for increases and decreases in visibility (e.g., due to cloud cover)  
141 relative to other years, which informs on our ability to perceive abrupt changes to the Earth's  
142 surface.

143 **Estimating archive completeness.** We quantified the 'completeness' of the Landsat  
144 archive as the proportion of usable images relative to an idealised expectation of one image  
145 taken every 16 days per active sensor (which is the typical recurrence). Here, the number of  
146 usable images corresponds to the sum of the annual quality-weighted frequencies. As a  
147 complement to this analysis, we counted the number of years without any satellite image data  
148 since 1982 to measure breaks in the continuity of Landsat.

149 **2.2. Analyses of effects of satellite data limitations on perceived land changes**

150 **Causal analysis approach.** We tested for biasing effects of data-quality on perceptions of  
151 land-change in three case studies. We tested for causal effects using Convergent Cross  
152 Mapping (CCM, Clark et al., 2015; Sugihara et al., 2012), a technique that can identify causal  
153 links between two temporal variables, even if these are not separable or if links are weak or  
154 nonlinear. To achieve this, CCM first constructs co-called 'shadow manifolds' of the two  
155 variables, which summarise their past behaviour over time. CCM then establishes whether  
156 there is a causal relationship between the variables by finding corresponding points in the

157 shadow manifolds of these variables (via “cross-mapping”), and testing whether the shadow  
158 manifolds ‘converge’, i.e., whether information from the causal variable has been embedded  
159 in the effect variable. The CCM outputs inform on the significance of the causal association,  
160 and on the ability of the causal variable to predict the outcome variable. The rationale for these  
161 tests is that a perceived land change is (by definition) biased if the presence of non-random  
162 data error (i.e., by spatial/temporal variation in our data-quality metrics) alters the specific  
163 nature of the change (e.g., its magnitude, timing, or direction).

164 In each study case, variables have varying and sometimes short time-series. We used an  
165 enhanced version of the original CCM method (Clark et al., 2015) that is robust to short time-  
166 series by applying dewdrop regression to combine information from multiple time-series. To  
167 this end, we ran the CCM analyses on a country-by-country basis, taking advantage of every  
168 relevant pixel within. We focused on causal effects detectable for these country-level  
169 aggregations, as this is the typical scale of SDG progress reporting (UNFCCC, 2015).

170 **Case study 1: Timing of deforestation.** We analysed data on the first year of deforestation  
171 between 1982 and 2021 from the Tropical Moist Forest dataset (Vancutsem et al., 2021). To  
172 align these data with our quality metrics, we aggregated them from their native 30-m resolution  
173 into a 1-km resolution by summing the corresponding pixel areas.

174 For an initial exploration of possible biases, we compared the directions of deforestation  
175 trends reported by national statistics (FAO, 2020) with the directions of country-level aggregate  
176 forest changes mapped by the TMF during the statistics’ respective reporting periods. To  
177 formally test for the presence of biases in the perceived forest changes, we used CCM (*see*  
178 *previous section*) to detect causal links between year-to-year changes in TMF-inferred  
179 deforestation rates and year-to-year changes in the maximum annual QI. Here, we hypothesised  
180 that improvements in data quality caused disproportionately high deforestation rates shortly  
181 after extended temporal gaps due to the backlog over data-limited year(s) during which no  
182 deforestation could be detected. To estimate year-to-year-changes in deforestation and data  
183 quality, we calculated positive/negative outliers for each of these variables based on the  
184 differences between annual values and their respective trendlines derived with Locally  
185 Weighted Scatterplot Smoothing (LOWESS, Seabold and Perktold, 2010), using a span of 0.4.  
186 We focused on pixel time-series experiencing  $\geq 1$  forest-cover change and  $\geq 1$  year without data.

187 **Case study 2: arable-land expansion.** We analysed a global dataset mapping the extent of  
188 arable-land for four-year epochs between 2000 and 2019 (GLAD, (Potapov et al., 2022)). To  
189 match these data to our quality metrics, we aggregated them from their native 30-m resolution  
190 to a 1-km resolution by the summing per-pixel areas.

191 To explore the potential existence of biases, we evaluated whether the GLAD-inferred  
192 gains/losses contradicted the directions of arable-land changes inferred from national statistics  
193 (FAO, 2023). For this, we conceptually aligned the FAO-reported arable-land areas to the  
194 GLAD by subtracting areas of temporary pastures and meadows (following the  
195 recommendation by FAO data experts for making these specific datasets comparable; Tubiello  
196 et al., 2023). We then aggregated the annual FAO values to per-epoch maximum areas per  
197 country. We chose maxima because the GLAD product maps any arable-land within a given  
198 epoch, making it sensitive to maximum extents.

199 To confirm the presence of data bias, we again used CCM. Here, we specifically evaluated  
200 whether the epoch-to-epoch time-series of GLAD-inferred arable-land gains that contradict  
201 FAO-inferred losses (i.e., the dominant form of disagreements; **Fig. 3c**) showed any causal  
202 signals of concurrent variations in quality-weighted Landsat image frequencies. For this, we  
203 recalculated the quality metrics per four-year epoch and aggregated them nationally,  
204 considering only pixels where the GLAD mapped arable-land at any point between 2000 and  
205 2019. Specifically, we here focused on pixels with both GLAD-inferred arable-land gains and  
206 increases in quality-weighted Landsat image frequencies.

207 **Case study 3: Seasonal surface-water gains.** We analysed changes in seasonal surface  
208 water based on the Global Surface Water dataset (GSW, Pekel et al., 2016). To assure the  
209 comparability of these data with our quality metrics, we aggregated the 30-m GSW to a 1-km  
210 resolution by summing per-pixel areas.

211 We first explored the possible existence of data biases by assessing the plausibility of long-  
212 term trends in seasonal surface-water amid in-situ evidence. For this, we compared GSW-  
213 inferred trends to river-discharge values measured at gauge stations (WMO, 2022). Because  
214 upstream surface water limits discharge (Duan et al., 2018), long-term changes in discharge  
215 should be correlated with upstream surface-water changes.

216 To enable this comparison, we took several steps to align both data sources. First, because  
217 the GSW maps seasonal water annually, we summarised the gauge station data to the same  
218 temporal resolution. For each station and year, we then estimated the annual range of discharge  
219 values. Larger ranges reflect either dry periods or periods of flooding, in both of which the  
220 GSW is expected to map seasonal water. Second, we estimated upstream seasonal-surface-  
221 water extents. For this, for each station and year, we used data on the connectivity of river  
222 flows within hydrological (sub-)basins (Lehner et al., 2008) to trace the upstream path most  
223 likely followed by water accumulated along a river. Here, we excluded gauge stations situated  
224 downstream of dams (using data by Mulligan et al., 2020). We did so to avoid misinterpreting  
225 any true disconnects between discharge and surface-water levels that may be caused by dams  
226 disrupting natural water flows. Additionally, at each gauge station, we did not compare  
227 discharge measurements against upstream seasonal-surface-water extents in years when the  
228 latter was estimated from groups of pixels containing missing values. Missing values appear in  
229 the GSW when water detection was avoided due to insufficient satellite observations. Upstream  
230 water extents represented by such pixels are likely to depict artificial and positive long-term  
231 trends due to gradual improvements in satellite data coverage and frequency, preventing an  
232 objective comparison with local discharge measurements.

233 These pre-processing steps preserved 3,917 stations. Then, we focused on the 4194 stations  
234 with a minimum of 8 data years (**Fig. S7a**) to enable subsequent smoothing. For each station,  
235 we smoothed their respective discharge and upstream surface-water time-series using  
236 LOWESS, and identified cases where both surface water and discharge experienced significant  
237 change trends using Mann-Kendall tests (Kendall, 1938;  $p < 0.05$ ). We restricted our  
238 comparison of the directions between discharge and surface-water trends to the 1,413 stations,  
239 where both trends were significant (**Fig. S7b**).

240 Additionally, we used CCM to formally test our hypothesis that changes in seasonal Landsat  
241 data completeness bias perceptions of changes in seasonal surface-water extents. Our

242 hypothesis is based on the premise that observing a pixel during extended periods of time  
243 within a given year increases the likelihood of detecting any short-lived seasonal water  
244 occurrences. Specifically, we tested for effects of positive/negative outliers in annual numbers  
245 of months with usable Landsat data on positive/negative outliers in seasonal surface-water  
246 areas. We detected outliers based on differences between annual values and LOWESS  
247 trendlines. We applied the CCM analysis separately for each country, focussing on pixels with  
248 seasonal surface water at any point during the observation period.

249 **Comparisons between lower- and higher-income countries.** We tested for asymmetries  
250 in the prevalence of confirmed biases in perceptions of land changes between higher- and  
251 lower-income regions of the world, as distinguished by World Bank data (Solt, 2020). For  
252 simplicity, we aggregated countries classified as either ‘low-income’ or ‘lower-middle-  
253 income’ into a ‘lower-income’ group, and those classified as either ‘upper-middle-income’ or  
254 ‘high-income’ into a ‘higher-income’ group.

255 To test for differences in the prevalence of bias in perceived land changes between lower-  
256 income and higher-income groups, we applied the McNemar test (McNemar, 1947) to  
257 frequencies of countries with significant causal effects vs. no effects in either group. To account  
258 for spatial autocorrelation, we matched each higher-income country to its spatially closest  
259 neighbour in the lower-income group, with replacement. The income-group comparisons for  
260 arable-land and surface-water changes thus had a sample size of 133 ( $N=133/83$  for  
261 higher/lower-income countries) and that for tropical-moist-forest changes a sample size of 41  
262 ( $N=36/41$  for higher/lower-income countries).

### 263 3. RESULTS AND DISCUSSION

#### 264 3.1. Spatial and temporal variations in data quality and coverage

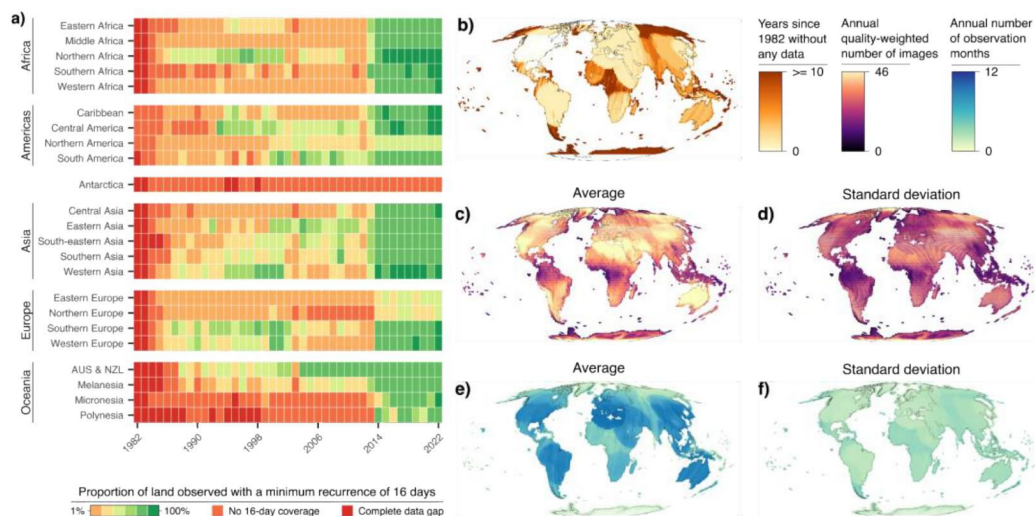
265 **An uneven history of satellite observations.** Between 1982 and 2022, the Landsat archive  
266 gathered 17,553,123 daytime images (average of 1,618 per 1-km pixel [ $\pm 1,599$ ], see **Fig. S1a**  
267 **in Supplementary Material**). This means that 33.1% of images possible under a 16-day revisit  
268 frequency are missing (see **Methods**). Moreover, the average 1-km pixel lost an additional  
269 44.8% of observations ( $\pm 17.6\%$ , **Fig. S1b/d**) due to quality issues such as clouds, haze, cloud  
270 shadows, or sensor degradation. This leaves an average of 1,429 images per pixel ( $\pm 887$ , **Fig.**  
271 **S1c**).

272 The global coverage of Landsat data evolved only gradually (**Fig. 2a**, **Fig. S3**) thanks to a  
273 network of receiving stations established in all continents except Antarctica (**Fig. S2a**).  
274 Whereas the archive grew by an average of 118,362 images per year during the 1980s  
275 ( $\pm 67,104$ ), this rate increased nearly five-fold by the 2010s (**Fig. S3**). However, improvements  
276 were not uniform. Many countries lacked (or still lack) the infrastructure and know-how to  
277 continuously collect and preserve data from overpassing satellites (Wulder et al., 2016, **Fig.**  
278 **S2a-b**), or to directly profit from centralised (but incomplete) online archives (SCU, 2022). As  
279 a result, many world regions, particularly at low and very high latitudes, have lagged behind in  
280 establishing coherent monitoring capabilities (**Fig. 2a**).

281 Despite gradual improvements, changes in satellite technologies caused several abrupt  
282 changes in data coverage. Since the launch of Landsat 7 in 1999, Landsat on-board data  
283 storages reduced the reliance on global networks of receiving stations for preserving data prior

284 to their archiving (Wulder et al., 2016). Combined with improvements in data transmission and  
 285 warehousing, this rapidly expanded the Landsat archive. Since 2003, however, mechanical  
 286 issues in Landsat 7 degraded as much as 25% of pixels per image (USGS, 2004). When Landsat  
 287 5 ended in 2010, available images were thus of poor quality. When Landsat 8 was launched in  
 288 2013, in turn, data coverage improved dramatically (**Fig. 2a**). The average proportion of  
 289 countries' lands with a 16-day coverage increased from 17.5% before 2013 ( $\pm 30.8\%$ ) to 89.4%  
 290 thereafter ( $\pm 26.4\%$ ). Yet, the interoperability between Landsat 8 and earlier missions was  
 291 hindered by differences in spectral information (Roy et al., 2016), a challenge not typically  
 292 addressed by state-of-the-art remote sensing products.

293 **Data limitations vary in space and time.** Except for much of North America, nearly all  
 294 lands have full-year interruptions in data coverage (**Fig. 2b**). Of these lands, 36.2% have  $\geq 1$ -  
 295 year interruptions after their first observation year, including most islands and most of Africa  
 296 (**Fig. S4a**). Often, these interruptions persisted for several years, leaving several Central  
 297 African regions without usable images during  $>10$  consecutive years (**Fig. S4b**). When data  
 298 are available, their frequency and quality vary (**Fig. 2c-d**). Much of the world has a large  
 299 number of *any* Landsat images (**Fig. S1a**), which is the metric commonly reported in  
 300 publications on new Landsat-based time-series products (e.g., Pekel et al., 2016; Potapov et al.,  
 301 2022; Vancutsem et al., 2021). Yet, only a relatively small, and non-random, subset of those  
 302 images have high quality. Consistently high coverages of high-quality images only exist for  
 303 dryland regions (**Fig. S1c**). In contrast, in most equatorial forest regions of the world, less than  
 304 half of existing images are usable due to persistent cloud cover (Ju and Roy, 2008) (**Fig. S1b**).  
 305 In addition, in areas such as the Sahel belt and Central Asia, annual fluctuations in quality-  
 306 weighted image frequencies exceed annual averages (**Fig. 2c-d**). Similarly, in those regions,  
 307 seasonal data coverages are highly incomplete, often with less than three data months in a given  
 308 year, and with fluctuations of a similar magnitude between years (**Fig. 2e-f**).

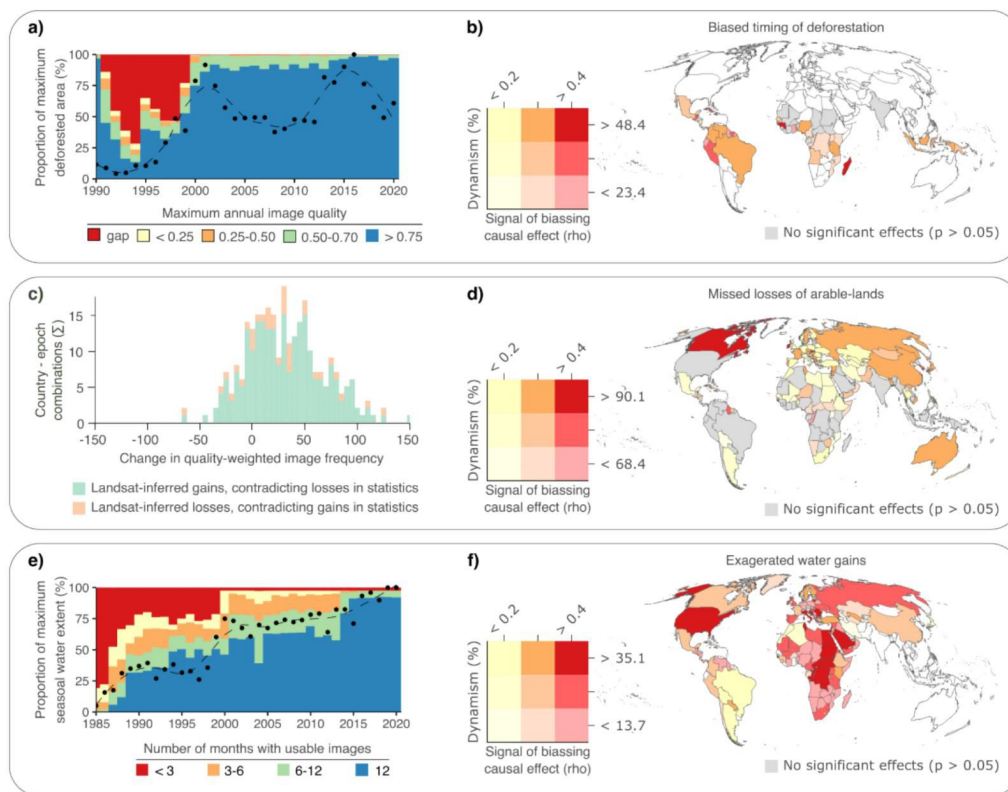


309  
 310 **Figure 2. Spatiotemporal variation in Landsat satellite data coverage and quality.** a) Year-to-year and regional variation  
 311 in proportions of land areas observed during every month of the year, highlighting both interruptions and gradual  
 312 improvements and a sharp increase in coverage in 2013, after the launch of Landsat 8. b) Accumulated  $\geq 1$ -year data gaps. c)  
 313 Global variation in average annual quality-weighted image numbers and d) their multiannual fluctuation. e) Global variation  
 314 in average annual numbers and f) multiannual fluctuation of observation months.



315 **3.2. Data limitations bias perceived changes in SDG indicators**

316 Temporal and spatial inconsistencies in Landsat data may, unless addressed, immediately  
 317 affect the monitoring of any land-change-related SDG. Data unevenness in earlier decades, too,  
 318 influences SDG monitoring, even if more indirectly. For example, in light of known data  
 319 constraints (ESA, 2020), the SDG monitoring framework has chosen 2000 as the baseline year  
 320 for measuring changes in extents of forests (indicator 15.1.1) and water-related ecosystems  
 321 (indicator 6.6.1). Yet, changes in greenhouse gas emissions (indicator 13.2.2), which depend  
 322 on both forest (Pearson et al., 2017) and wetland extents (Zhang et al., 2017), are generally  
 323 evaluated against a 1990 baseline (UN DESA, 2022). Long-term, temporally consistent time-  
 324 series products are thus needed, to not only meet the specific monitoring needs for individual  
 325 SDG indicators, but also to assure that monitoring across SDGs is coherent, and that systemic  
 326 interrelations between SDGs are adequately captured. However, as we demonstrate in the  
 327 following three case studies, data limitations distort our perception of changes in several SDG  
 328 indicators.



329 **Figure 3. Effects of satellite data limitations on perceived land changes.** a) Points: annual lost tropical moist forest areas  
 330 normalised by the maximum extent, revealing positive/negative outliers relative to smoothed trend (LOWESS with 0.4 span;  
 331 dashed line). Colours indicate percentages of forest extent observed with different maximum annual data qualities. b) Country-  
 332 level differences in evidence of biasing causal effects ( $\rho$ ; x-axis), compared to proportions of the maximum forest extent  
 333 experiencing changes (hereafter ‘dynamism’; y-axis). c) Frequency of disagreements in the direction of Landsat-inferred  
 334 arable-land losses/gains between mapped 4-year epochs and changes derived from official statistics, distributed along a  
 335 gradient of changes in quality-weighted Landsat image frequencies between epochs. Country-level contributions to the  
 336 histograms are weighted by information on national statistical reporting performances (World Bank, 2021). d) is similar to b),  
 337 but measures effects of improvements in Landsat data quality on Landsat-inferred gains in arable-land that contradict statistics-  
 338 inferred losses. e) Analogous to a), points indicate the annual and global seasonally inundated areas, normalised to maximum  
 339 extent, and colours indicate percentages of the maximum extent observed with varying seasonal Landsat data completeness.  
 340 f) is as b), but for effects of anomalies in completeness on anomalies in seasonal water areas.  
 341

342 **Case study 1: Gaps in quality data bias perceived timings of deforestation events.**  
343 Changes in forest areas are the focus of SDG indicator 15.1.1. Tropical moist forests, in  
344 particular, accounted for >90% of global deforestation since 2000 (FAO, 2020) and are vital  
345 carbon sinks (SDG 13) and biodiversity refuges (SDG 15) that provide billions of people with  
346 income, food, and medicine (SDGs 1, 2, and 3). Accordingly, the recently published Landsat-  
347 based Tropical Moist Forest product (TMF, Vancutsem et al., 2021) is poised to play a  
348 prominent role in global SDG monitoring.

349 The TMF tackles gaps in Landsat data by handling temporal data for each pixel  
350 independently. Forest cover and change are classified continuously. Then, by assuming change  
351 is absent if not observable, a seemingly annual time-series is generated. Yet, given that data  
352 quality and coverage vary in time and space, the true timing of forest-change events is often  
353 uncertain. Accordingly, change magnitudes can be overestimated following data gap years, or  
354 in years when high image frequencies are needed to track progressive change events such as  
355 creeping deforestation.

356 We examined the TMF and, indeed, found indications of such biases. We registered  
357 unusually extensive deforestation rates during two periods since 1990, both marked by rapid  
358 improvements in the Landsat archive (**Fig 3a**). From 1999 to 2000, right after the launch of  
359 Landsat 7, we noted a 65.2% increase in deforestation, more than twice the maximum year-  
360 over-year increase (31.9%) between 1990 and 1999. Similarly, the 2012-2013 deforestation  
361 increase of 60.5% coincides with higher image frequencies following the launch of Landsat 8.  
362 This is nearly twice the recorded maximum between 2001 and 2012 (30.8%) when Landsat 7  
363 was the main source of data, despite its continued degradation since 2003. Where data was  
364 absent or potentially unusable for  $\geq 1$ -year, we found higher deforestation immediately  
365 following such gaps (**Fig. 3a**; *see Methods*). Overall, we found that 58.4% of deforestation  
366 mapped since 1990 follow periods with no data, and are thus potentially allocated to wrong  
367 years (**Fig. S5a**; *see Methods*).

368 To confirm whether data limitations influenced our perception of the timing of  
369 deforestation, we used a formal causal analysis technique developed for detecting causal  
370 relationships between two time-series called Convergent Cross Mapping (CCM, Clark et al.,  
371 2015; Sugihara et al., 2012; *see Methods*). This technique allowed us to identify cases where  
372 perceived changes are biased because some components of those changes (e.g., their  
373 magnitudes or directions) are in part caused by variation in the observation process (i.e., in data  
374 coverage and/or quality).

375 Based on this analysis, we found that deforestation anomalies can be partially attributed to  
376 those in maximum annual image quality in 68.8% of tropical-moist-forest countries (**Fig. 3b**;  
377 *see Methods*). The distorted perceptions of deforestation years may bias timing-sensitive  
378 applications related to SDGs, including modelling of carbon emissions (IPCC et al., 2019) and  
379 extinction debts (Figueiredo et al., 2019), or attributions of forest changes to socio-political  
380 conditions (Nackoney et al., 2014). For example, deforestation inside the Luo Scientific  
381 Reserve (Democratic Republic of Congo), that reportedly happened during the first Congo war  
382 (1996-1997) due to human displacement (Nackoney et al., 2014), would be falsely attributed  
383 to processes in the immediate post-war period when Landsat data were again available  
384 following a multi-year data gap (**Fig. S5b**).

385 These biases may also cast unfair perceptions of progress in curbing deforestation. For  
386 example, twelve countries indicated by the TMF as having increasing deforestation rates  
387 around the Landsat 8 launch reported decreasing trends relative to the previous reporting period  
388 (Keenan et al., 2015), although we stress that due to conceptual differences, these changes are  
389 not directly comparable (Chazdon et al., 2016). These include countries experiencing forest  
390 transitions and/or that are recognized for their long-term progress in forest restoration (e.g.,  
391 Cuba, Goulart et al., 2018).

392 **Case study 2: Increasing frequencies of quality data miss regional arable-land losses.**  
393 Accurate data on arable-land extents are essential for mapping agricultural lands under  
394 sustainable use (indicator 2.4.1), and are also closely linked to indicators on deforestation  
395 (15.2.1) and on losses of water-related ecosystems (6.6.1, UN DESA, 2022).

396 Mapping arable land requires a dense time-series. This enables detecting changes driven by  
397 planting and harvesting, which help improve mapping accuracies (Fan et al., 2022) but may be  
398 overlooked due to gaps in the Landsat archive. To tackle this issue, a recently developed global  
399 product (GLAD, Potapov et al., 2022) maps arable-land in four-year epochs, exploiting all  
400 images in an entire epoch to more accurately characterise crop phenology. Although this  
401 precludes shorter-term change assessments, it is a necessary compromise. Yet, this approach is  
402 not immune to year-to-year improvements in high-quality image frequencies (**Fig. S3**). These  
403 improvements increase the detectability of key intra-annual changes related to land  
404 management, and may thus lead to overestimations of arable-land gains.

405 We examined the GLAD for indications of change biases. To this end, we compared national  
406 aggregates of the GLAD against corresponding FAO statistics on arable-lands. We adjusted  
407 the latter following expert recommendations to conceptually match these data with the GLAD  
408 (Tubiello et al., 2023). We identified 123 suspicious-looking countries where mapped gains  
409 contrasted with reported losses (**Fig. S6**). This relates to arable-land expansions in >800 million  
410 30-m pixels, more than the combined number of arable-land pixels of all Amazonian countries  
411 in 2021 (FAO, 2023, **Fig. S5c**).

412 Disagreements peaked between the 2008-2011 and 2012–2015 epochs (36.0% of cases).  
413 The first peak coincides with the discontinuation of Landsat 5 in 2010, when parallelly captured  
414 Landsat 7 images were heavily degraded, causing an abrupt decrease in data frequencies. The  
415 second peak coincides with the launch of Landsat 8 in 2013, which led to a massive increase  
416 in data frequencies and moreover marked a shift in sensing technologies. Compared to previous  
417 sensors, Landsat 8 provides data for different spectral ranges (Roy et al., 2016). We found no  
418 indication that the GLAD is corrected for these issues.

419 Naturally, cases of GLAD-FAO disagreements alone do not provide evidence of biases in  
420 GLAD-inferred change perceptions, as they might equally reflect known errors in FAO data  
421 (See et al., 2015). To identify those cases where changes are demonstrably caused by the  
422 GLAD's underlying observation process, we again used CCM (*see Methods*). Focusing on  
423 countries with positive disagreements (i.e., where GLAD mapped gains instead of losses), our  
424 analysis confirmed that, for 48.4% of countries in this category, changes in quality-weighted  
425 image frequencies not only contribute to causing perceived arable-lands changes, but can also  
426 predict the temporal patterns of the latter (**Fig. 3d**). These include top food-producing countries  
427 that together accounted for 38.4% of the global cereal production in 2021 (World Bank, 2023),

428 including several that are well-known for their large arable-land losses (e.g., China,  
429 Bangladesh, Canada). They also include food-insecure countries (e.g., Yemen, Zimbabwe),  
430 where misinterpreting losses of arable lands as gains could misinform policy-makers on  
431 emerging crises.

432 Overestimated arable-land gains can also lead to unfair evaluations of progress towards  
433 SDG target 2.4 (sustainable food production) by exaggerating conflicts of food security with  
434 ecosystem protection and climate-change mitigation. For example, two recent studies using  
435 GLAD data (Meng et al., 2023; Wang et al., 2023) reported extensive cropland expansion into  
436 global protected areas that massively accelerated between the mid-2000s and mid-2010s. The  
437 above-described data biases surrounding the 2013 launch of Landsat 8 (**Fig. 2a**, **Fig. 3c**),  
438 however, may render these assessments unreliable. This is illustrated in India, where sudden  
439 changes in Landsat data apparently led the GLAD to misinterpret wetland pixels as arable-  
440 lands, leading to the false mapping of agricultural conversion over an entire Ramsar wetland  
441 of >3,000 ha (**Fig. S5d**).

442 **Case study 3: Improving seasonal data completeness exaggerates water gains.** SDG  
443 Indicator 6.6.1 tracks changes in surface water bodies, such as lakes, rivers, and reservoirs, for  
444 which the Landsat-based Global Surface Water product (GSW, Pekel et al., 2016) provides  
445 critical input. In particular, the GSW's ability to depict seasonal water occurrences is crucial  
446 for sustainability questions. In many dryland regions, seasonal water bodies lasting a few  
447 months per year support food and water security for people and livestock (Michalak et al.,  
448 2023). Additionally, even outside drylands, seasonal flooding of river plains affects nutrient  
449 inputs in, and leaching from, major agricultural regions (Talbot et al., 2018).

450 The GSW classifies water occurrences monthly. Then, it distinguishes seasonal from  
451 permanent water annually based on interruptions in the monthly occurrences. The authors of  
452 the GSW accounted for temporal inconsistencies in the Landsat archive by only classifying  
453 pixels with  $\geq 10$  observations. This reduces some bias without precluding global mapping.  
454 However, the nearly 5-fold increase in seasonal water mapped by the GSW between 1984 and  
455 2020, with positive trends over 90.1% of the maximum seasonal-water extent, cannot be  
456 disconnected from data improvements. Specifically, because the GSW maps water if as little  
457 as 43.5% of the expected annual number of images are available, seasonally biased  
458 distributions of those images could miss seasonal water occurrences, or misclassify seasonal  
459 for permanent water (if only covering dry or wet seasons, respectively). Therefore,  
460 improvements in data completeness (i.e., number of months with usable data) could be falsely  
461 mapped as seasonal-water gains (Yamazaki and Trigg, 2016).

462 We found that, indeed, global seasonal surface-water gains strongly correlate with  
463 improvements in seasonal data completeness ( $r^2=0.80$ ; **Fig. 3e**) and are often unsupported by  
464 local discharge measurements (90.7% of gauge stations with significant long-term changes  
465 showed disagreements, **Fig. S7**; see *Methods*). Using CCM, we found that changes in seasonal  
466 data completeness contributed to causing perceived changes in seasonal surface water in 144  
467 countries, with moderate to high predictive power (**Fig. 3f**). These countries include several  
468 with severe water stress (e.g., Yemen, Sudan, World Bank, 2023), where mapping false  
469 seasonal-water gains and losses could potentially result in drastic mischaracterizations of  
470 water-related sustainability issues.

471 In all the three cases discussed here, we cannot ascertain whether any specific pixel-level  
472 changes under suspicion are actually false, nor that any perceived changes exclusively, or even  
473 primarily, originate from data limitations. However, our results show that year-to-year  
474 variations in data coverage and/or quality contribute to causing perceived year-to-year land  
475 changes, and that we would not have perceived changes of the same nature and/or magnitude  
476 without changes in data quality. Although we demonstrate these issues with a focus on Landsat  
477 data, they are expected to apply similarly to other satellite data archives used in global land-  
478 change monitoring (e.g., AVHRR, MODIS, Sentinel), given that those, too, are uneven in their  
479 data coverage and quality (Dech et al., 2021; Justice et al., 2002; Sudmanns et al., 2020).

### 480 **3.3. Biases disproportionately affect lower-income countries**

481 Monitoring data that are consistent (and thus comparable) in space and time are essential to  
482 support international SDG-related policymaking that is both equitable across boundaries (Xu  
483 et al., 2020) and fair in acknowledging the historical development of national issues (Coolsaet  
484 and Pitseys, 2015). Yet, our results call into question whether contemporary Landsat-based  
485 monitoring can really provide fair support, as biasing effects of data limitations are highly  
486 uneven across countries. Notably, countries with limited financial capacities to produce  
487 independent, higher-quality monitoring data that might counter perceptions based on global  
488 satellites are more strongly affected by biases in the latter. Specifically, we found that biasing  
489 effects on perceived arable-land and seasonal-water trends were significantly more frequent in  
490 lower-income than in higher-income countries (McNemar's tests, arable-land: 51.9% of lower-  
491 income vs. 46.1% of higher-income,  $p<0.05$ ; water: 89.7% vs. 73.1%,  $p<0.05$ ; note there was  
492 a near-significant difference in deforestation bias in the opposite direction among the respective  
493 income groupings of tropical-moist-forest countries; 51.9% vs. 46.1%,  $p=0.07$ ; *details in*  
494 *Methods*).

495 The geographical biases in land-change perceptions may contribute to distorted or  
496 unbalanced narratives about sustainability challenges between lower- and higher-income  
497 countries. In the worst case, misperceptions of progress towards food- and water-security goals  
498 in lower-income countries, that in reality reflect improvements over initially more limited data,  
499 might hamper adequate international support and timely policy interventions. Risks of such  
500 misinterpretations seem particularly high when comparing progress against pre-2013 baselines,  
501 after which Landsat 8 offered substantially improved spatial and temporal data coverage.

### 502 **3.4. Future needs: bias corrections, fair product validations, and support to users**

503 The data limitations we demonstrated are being acknowledged in the remote sensing  
504 community (Frantz et al., 2023; Lewińska et al., 2023; Zhang et al., 2022) and commonly  
505 discussed in published materials describing new data products. For example, the authors of the  
506 TMF discuss how observation frequencies affect the detection of deforestation, and those of  
507 the GSW discuss difficulties in detecting water due to varying data completeness. However,  
508 these fundamental issues are typically discussed only swiftly and in general terms. Those  
509 discussions may resonate with remote sensing experts, who are closely familiar with them. By  
510 contrast, for many non-expert data users, the eye-popping advances achieved through legacy  
511 programs such as Landsat can lend any product derived with it an appearance of high quality,  
512 driving data choices and overconfident uses (Molder et al., 2022). Given the central role of

513 satellite-based land-change observations in sustainability policy, monitoring, and related  
514 scientific fields, it is imperative that we take our collective management of data limitations to  
515 a whole new level. To this end, several steps can be taken by both expert and non-expert  
516 communities to improve the usability, interpretability, and sound application of remote-  
517 sensing-based data products, including more rigorous bias-controls by data developers, as well  
518 as support for (and commitment by) data users to detect and address uncertainties.

519 **Improving the handling and reporting of data uncertainties and biases.** Some of the data  
520 issues we described can be tackled by raising standards for correcting for satellite data  
521 limitations before developing products. For example, methods to correct for spectral  
522 differences between Landsat sensors – which likely explain some abrupt year-to-year changes  
523 in Landsat-based data products – are readily available (Che et al., 2021; Roy et al., 2016).  
524 Although some developers already use such methods (Gong et al., 2020; Senf and Seidl, 2021),  
525 this remains rare. Additionally, an increasing array of approaches can fill gaps in satellite  
526 archives (Asare et al., 2020; Yin et al., 2017), for instance, by fusing sparse Landsat data with  
527 coarser-resolution but less incomplete data from MODIS and AVHRR sensors to generate  
528 global, seamless data cubes (as showcased by Liu et al., 2021). Naturally, such methods carry  
529 their own uncertainties, and their effectiveness likely depends on the severity of satellite data  
530 limitations.

531 Additionally, we need higher standards for validating remote sensing data products. We  
532 recognize that the products analysed here were, in fact, extensively validated. In addition, the  
533 most recent ones follow current best practices in sample-based estimations of map accuracies  
534 and uncertainties (Olofsson et al., 2014). However, even current best practices do not account  
535 explicitly for gradients in satellite data quality and coverage. This is problematic because  
536 limitations in satellite images can not only locally reduce the performance of classification  
537 algorithms, but also impede the accurate visual interpretation of images. Yet, global, multi-  
538 decadal products (including those analysed here) are typically validated against reference  
539 samples derived by visually interpreting Landsat images, especially for pre-2000 periods,  
540 where few alternative sources of validation data exist (Chazdon et al., 2016). As a result, the  
541 very pixels and years when classification algorithms are most likely to fail may either be  
542 systematically underrepresented by validation samples (as samples there are less likely  
543 accepted as ‘validation-grade’), and/or their samples’ labels may include more errors. This  
544 means that reported accuracy scores may not be generalizable to the complete maps, and may  
545 in the worst case exaggerate true accuracies, even if developers otherwise followed best  
546 practices regarding spatiotemporally and environmentally representative sampling (Olofsson  
547 et al., 2014).

548 To tackle such spatial and temporal biases when validating remote sensing data products,  
549 predictive models could be used to probabilistically estimate class-confusion probabilities  
550 beyond the validation samples. Such models could directly account for different sources of bias  
551 in relevant observation processes, for example, by incorporating covariates capturing the  
552 quality of the satellite data underpinning image-derived reference samples, factors limiting the  
553 collection of samples in the field (e.g., accessibility), and environmental factors linked to  
554 varying performance of classification algorithms (e.g., topography). As a result, the modelled,  
555 contiguous probability estimates would offer a more representative basis for calculating

556 accuracy scores for any given region of interest than the raw validation samples. Remote  
557 sensing has a rich set of tools to minimise data biases as far as possible (e.g., gap filling,  
558 randomised sampling; Asare et al., 2020; Olofsson et al., 2014). In turn, other fields in which  
559 data are usually highly biased have developed long traditions of developing models to explicitly  
560 account for sampling biases (e.g., ecology, Chadwick et al., 2023; Chauvier et al., 2021; Fink  
561 et al., 2023, hydrology, Rasmussen et al., 2016). Integrating approaches from these fields could  
562 substantially improve the robustness of accuracy reporting (Simmonds et al., 2022).

563 Beyond the immediate benefits through enabling more reliable accuracy assessments, the  
564 modelling of contiguous uncertainties can also help empower data users to better address  
565 remaining data limitations in their applications. This is especially so, if the contiguous  
566 uncertainties are provided in ways that enable efficient uptake in commonly used downstream  
567 analysis frameworks (e.g., via probabilistic sampling in Bayesian analyses, or via weighting of  
568 input data in Machine Learning). For example, mapping products showing per-pixel  
569 probability-mass functions of different classes would make it much easier for product users to  
570 derive unbiased area estimations over larger regions, compared to the classical way of mapping  
571 just the highest-probability class per pixel. Similarly, per-pixel probability-mass functions of  
572 alternative temporal class sequences could readily be propagated into change analyses and  
573 indicators (Kirchner et al., 2021; Rowland et al., 2021).

574 All these measures would imply more time needed for the development and quality-  
575 assurance of these products, and thus likely lead to fewer products entering the market  
576 following peer-review. This would be desirable from the perspective of data users, who are  
577 already overwhelmed by too many products to choose from, with little guidance on which ones  
578 to trust.

579 **Helping users select fit-for-purpose data products.** To promote sensible uses of time-  
580 series products, we must acknowledge that many users have little to no training in remote  
581 sensing. Such users require support both in selecting the most adequate products and in  
582 understanding the implications of those products' uncertainties for their desired applications.

583 One way to provide such support could be through cloud-based tools that automatically  
584 identify candidate products for a given user-specified application. Such tools can  
585 simultaneously assess where within a specified region and period each product could plausibly  
586 support this application, given limitations in the products' underlying satellite data. To interpret  
587 the users' descriptions of their applications and translate those into targeted product queries,  
588 such tools could draw on Large Language models (LLMs; as demonstrated by Li and Zhang,  
589 2023). LLMs could be pre-trained on expert literature on both the data requirements of common  
590 application types (e.g., temporal consistency for change analyses) and on the satellite-data  
591 requirements for mapping different variables. For example, literature shows that mapping  
592 arable-lands is best achieved with satellite observations made during periods of key  
593 management interventions such as sowing and harvesting (Fan et al., 2022; Prishchepov et al.,  
594 2012). Information on these periods obtained from regional crop calendars (Belén Franch and  
595 Whitcraft, 2022), and provenance metadata on the candidate products' satellite-data inputs  
596 (Fischer et al., 2023) could be integrated with customised satellite-data-quality metrics (e.g.,  
597 measuring the quality of images over target dates) to perform data queries. Summaries of the  
598 test's results and rationales, the recommended product(s), and areas/periods where the

599 application is likely to be unreliable could be communicated to users via automatically  
600 generated light-weight reports.

601 Data queries and reports will require metrics of data quality and availability that can  
602 effectively guide product selections while considering application-specific data requirements.  
603 While the data-quality metrics analysed here are broadly relevant for different applications in  
604 land-change monitoring, certain applications will require custom metrics. Existing literature on  
605 specialised remote sensing applications can provide guidance for constructing such metrics  
606 (e.g., Fan et al., 2022; Mas and Soares de Araújo, 2021; Prishchepov et al., 2012; Vaudour et  
607 al., 2019). For instance, in temperate regions, image composites centred around phenological  
608 peaks are relevant for forest monitoring, and data frequencies estimated within those temporal  
609 windows would be most informative (Lewińska et al., 2023). In other cases, further research  
610 into application-specific data requirements may still be needed before adequate metrics to  
611 measure data limitations can be conceived (e.g., land-surface mapping in mountain regions  
612 (Vanonckelen et al., 2014).

613 **Towards responsible uses of data products.** Clearly, there is a need, and opportunity, for  
614 better data products, data-quality information, and support tools. Ultimately, however, none of  
615 those can take away the responsibility of data users' for ensuring that the used data products  
616 are fit-for-purpose for their specific applications, nor for evaluating the plausibility of their  
617 studies' original results. Often, steps as simple as skimming through contextually relevant  
618 literature or visually exploring historical high-resolution images (e.g., using Google Earth) can  
619 already reveal issues (e.g., as demonstrated in **Fig. S5**). Similarly, regional bar plots of annual  
620 areas often suffice to reveal suspicious-looking anomalous trends in time series products that  
621 warrant further scrutiny.

622 Optimally, data users of remote sensing products would explore causal associations between  
623 target variables and satellite data-quality metrics. Here, effect-size measures (e.g., combining  
624 CCM with S-Map, Deyle et al., 2016) may be used to evaluate whether the magnitudes of any  
625 identified biasing effects driven by data-quality limitations are tolerable, given the studies'  
626 specific goals and conclusions. Users interested in Landsat-based products may integrate our  
627 quality metrics in such analyses. However, we caution that we designed our layers (*see Data*  
628 *availability*) to measure broad-scale variations in data availability and quality. Those  
629 differences are captured effectively by focusing on the issues recorded during the sensing  
630 process. These reflect both constrained visibility (directly by clouds, and indirectly by cloud  
631 shadows and haze), technical sensing issues (related to atmospheric corrections,  
632 orthorectification, and sensor degradation), and data losses. Users interested in finer-scale  
633 inferences should instead compute our quality metrics using the available pixel-level metadata,  
634 and also incorporate the modelled, pixel-level information on clouds, cloud shadows, and  
635 atmospheric opacity that accompanies each Landsat acquisition. We caution, however, that the  
636 algorithms used to model the latter may not be universally reliable (Foga et al., 2017; Skakun  
637 et al., 2022).

#### 638 4. CONCLUSIONS

639 While Landsat satellite data are vital for sustainability monitoring, their uneven coverage  
640 and quality extends into derived monitoring products. This can bias perceptions of changes in



641 ecosystems, food, and water resources, particularly impacting less developed nations.  
642 Recognition of these limitations and efforts to address them are needed by both data developers,  
643 data users, and developers of support tools. Data developers are best positioned to attenuate the  
644 imprint of input data limitations on their products, and to improve transparency on remaining  
645 uncertainties. In turn, data users are ultimately responsible for choosing appropriate products  
646 and for assuring the soundness of any conclusions made through them. Shared ownership of  
647 the problem by different stakeholders is an essential step in assuring robust change assessments  
648 in order to promote responsible policy decisions.

## 649 REFERENCES

- 650 1. Anderson, K., Ryan, B., Sonntag, W., Kavvada, A., Friedl, L., 2017. Earth observation in  
651 service of the 2030 Agenda for Sustainable Development. *Geo-Spat. Inf. Sci.* 20, 77–96.  
652 <https://doi.org/10.1080/10095020.2017.1333230>
- 653 2. Asare, Y.M., Forkuo, E.K., Forkuor, G., Thiel, M., 2020. Evaluation of gap-filling methods  
654 for Landsat 7 ETM+ SLC-off image for LULC classification in a heterogeneous landscape  
655 of West Africa. *Int. J. Remote Sens.* 41, 2544–2564.  
656 <https://doi.org/10.1080/01431161.2019.1693076>
- 657 3. Belén Franch, Z.S., Juanma Cintas, Inbal Becker-Reshef, María José Sanchez-Torres, Javier  
658 Roger, Sergii Skakun, José Antonio Sobrino, Kristof Van Tricht, Jeroen Degerickx, Sven  
659 Gilliams, Benjamin Koetz, Whitcraft, A., 2022. Global crop calendars of maize and wheat  
660 in the framework of the WorldCereal project. *GIScience Remote Sens.* 59, 885–913.  
661 <https://doi.org/10.1080/15481603.2022.2079273>
- 662 4. Chadwick, F.J., Haydon, D.T., Husmeier, D., Ovaskainen, O., Matthiopoulos, J., 2023.  
663 LIES of omission: complex observation processes in ecology. *Trends Ecol. Evol.*  
664 <https://doi.org/10.1016/j.tree.2023.10.009>
- 665 5. Chauvier, Y., Zimmermann, N.E., Poggiato, G., Bystrova, D., Brun, P., Thuiller, W., 2021.  
666 Novel methods to correct for observer and sampling bias in presence-only species  
667 distribution models. *Glob. Ecol. Biogeogr.* 30, 2312–2325.  
668 <https://doi.org/10.1111/geb.13383>
- 669 6. Chazdon, R.L., Brancalion, P.H.S., Laestadius, L., Bennett-Curry, A., Buckingham, K.,  
670 Kumar, C., Moll-Rocek, J., Vieira, I.C.G., Wilson, S.J., 2016. When is a forest a forest?  
671 Forest concepts and definitions in the era of forest and landscape restoration. *Ambio* 45,  
672 538–550. <https://doi.org/10.1007/s13280-016-0772-y>
- 673 7. Che, X., Zhang, H.K., Liu, J., 2021. Making Landsat 5, 7 and 8 reflectance consistent using  
674 MODIS nadir-BRDF adjusted reflectance as reference. *Remote Sens. Environ.* 262, 112517.  
675 <https://doi.org/10.1016/j.rse.2021.112517>
- 676 8. Clark, A.T., Ye, H., Isbell, F., Deyle, E.R., Cowles, J., Tilman, G.D., Sugihara, G., 2015.  
677 Spatial convergent cross mapping to detect causal relationships from short time series.  
678 *Ecology* 96, 1174–1181. <https://doi.org/10.1890/14-1479.1>
- 679 9. Claverie, M., Ju, J., Masek, J.G., Dungan, J.L., Vermote, E.F., Roger, J.-C., Skakun, S.V.,  
680 Justice, C., 2018. The Harmonized Landsat and Sentinel-2 surface reflectance data set.  
681 *Remote Sens. Environ.* 219, 145–161. <https://doi.org/10.1016/j.rse.2018.09.002>
- 682 10. Coolsaet, B., Pitseys, J., 2015. Fair and Equitable Negotiations? African Influence and  
683 the International Access and Benefit-Sharing Regime. *Glob. Environ. Polit.* 15, 38–56.

- 684 [https://doi.org/10.1162/GLEP\\_a\\_00297](https://doi.org/10.1162/GLEP_a_00297)
- 685 11. Cracknell, A.P., 2018. The development of remote sensing in the last 40 years. *Int. J.*  
686 *Remote Sens.* 39, 8387–8427. <https://doi.org/10.1080/01431161.2018.1550919>
- 687 12. Dech, S., Holzwarth, S., Asam, S., Andresen, T., Bachmann, M., Boettcher, M., Dietz,  
688 A., Eisfelder, C., Frey, C., Gesell, G., Gessner, U., Hirner, A., Hofmann, M., Kirches, G.,  
689 Klein, D., Klein, I., Kraus, T., Krause, D., Plank, S., Popp, T., Reinermann, S., Reiners, P.,  
690 Roessler, S., Ruppert, T., Scherbachenko, A., Vignesh, R., Wolfmüller, M., Zwenzner, H.,  
691 Kuenzer, C., 2021. Potential and Challenges of Harmonizing 40 Years of AVHRR Data:  
692 The TIMELINE Experience. *Remote Sens.* 13, 3618. <https://doi.org/10.3390/rs13183618>
- 693 13. Deyle, E.R., May, R.M., Munch, S.B., Sugihara, G., 2016. Tracking and forecasting  
694 ecosystem interactions in real time. *Proc. R. Soc. B Biol. Sci.* 283, 20152258.  
695 <https://doi.org/10.1098/rspb.2015.2258>
- 696 14. Duan, K., Sun, G., Caldwell, P.V., McNulty, S.G., Zhang, Y., 2018. Implications of  
697 Upstream Flow Availability for Watershed Surface Water Supply across the Conterminous  
698 United States. *JAWRA J. Am. Water Resour. Assoc.* 54, 694–707.  
699 <https://doi.org/10.1111/1752-1688.12644>
- 700 15. ESA, 2020. Compendium of Earth Observation contributions to the SDG Targets and  
701 Indicators, Earth Observation for SDG. European Space Agency (ESA), Rome, Italy.
- 702 16. Fan, L., Yang, J., Sun, X., Zhao, F., Liang, S., Duan, D., Chen, H., Xia, L., Sun, J.,  
703 Yang, P., 2022. The effects of Landsat image acquisition date on winter wheat classification  
704 in the North China Plain. *ISPRS J. Photogramm. Remote Sens.* 187, 1–13.  
705 <https://doi.org/10.1016/j.isprsjprs.2022.02.016>
- 706 17. FAO, 2023. FAOSTAT statistical database [WWW Document]. URL  
707 <https://www.fao.org/faostat/> (accessed 3.7.23).
- 708 18. FAO, 2020. Global Forest Resources Assessment 2020. FAO, Rome, Italy.
- 709 19. Figueiredo, L., Krauss, J., Steffan-Dewenter, I., Sarmiento Cabral, J., 2019.  
710 Understanding extinction debts: spatio-temporal scales, mechanisms and a roadmap for  
711 future research. *Ecography* 42, 1973–1990. <https://doi.org/10.1111/ecog.04740>
- 712 20. Fink, D., Johnston, A., Strimas-Mackey, M., Auer, T., Hochachka, W.M., Ligocki, S.,  
713 Oldham Jaromczyk, L., Robinson, O., Wood, C., Kelling, S., Rodewald, A.D., 2023. A  
714 Double machine learning trend model for citizen science data. *Methods Ecol. Evol.* 14,  
715 2435–2448. <https://doi.org/10.1111/2041-210X.14186>
- 716 21. Fischer, J., Egli, L., Groth, J., Barrasso, C., Ehrmann, S., Figgemeier, H., Henzen, C.,  
717 Meyer, C., Müller-Pfefferkorn, R., Rümmler, A., Wagner, M., Bernard, L., Seppelt, R.,  
718 2023. Approaches and tools for user-driven provenance and data quality information in  
719 spatial data infrastructures. *Int. J. Digit. Earth* 16, 1510–1529.  
720 <https://doi.org/10.1080/17538947.2023.2198778>
- 721 22. Foga, S., Scaramuzza, P.L., Guo, S., Zhu, Z., Dilley, R.D., Beckmann, T., Schmidt,  
722 G.L., Dwyer, J.L., Hughes, M.J., Laue, B., 2017. Cloud detection algorithm comparison and  
723 validation for operational Landsat data products. *Remote Sens. Environ.* 194, 379–390.  
724 <https://doi.org/10.1016/j.rse.2017.03.026>
- 725 23. Frantz, D., Rufin, P., Janz, A., Ernst, S., Pflugmacher, D., Schug, F., Hostert, P., 2023.  
726 Understanding the robustness of spectral-temporal metrics across the global Landsat archive  
727 from 1984 to 2019 – a quantitative evaluation. *Remote Sens. Environ.* 298, 113823.

- 728 <https://doi.org/10.1016/j.rse.2023.113823>
- 729 24. Gong, P., Li, X., Wang, J., Bai, Y., Chen, B., Hu, T., Liu, X., Xu, B., Yang, J., Zhang,  
730 W., Zhou, Y., 2020. Annual maps of global artificial impervious area (GAIA) between 1985  
731 and 2018. *Remote Sens. Environ.* 236, 111510. <https://doi.org/10.1016/j.rse.2019.111510>
- 732 25. Goulart, F., Galán, Á.L., Nelson, E., Soares-Filho, B., 2018. Conservation lessons from  
733 Cuba: Connecting science and policy. *Biol. Conserv.* 217, 280–288.  
734 <https://doi.org/10.1016/j.biocon.2017.10.033>
- 735 26. Gregory, S., Hulse, D., Bertrand, M., Oetter, D., 2012. The Role of Remotely Sensed  
736 Data in Future Scenario Analyses at a Regional Scale, in: *Fluvial Remote Sensing for  
737 Science and Management*. John Wiley & Sons, Ltd, pp. 271–297.  
738 <https://doi.org/10.1002/9781119940791.ch12>
- 739 27. Gustafson, A., Rice, R.E., 2020. A review of the effects of uncertainty in public science  
740 communication. *Public Underst. Sci.* 29, 614–633.  
741 <https://doi.org/10.1177/0963662520942122>
- 742 28. Hansen, M.C., Potapov, P.V., Moore, R., Hancher, M., Turubanova, S.A., Tyukavina,  
743 A., Thau, D., Stehman, S.V., Goetz, S.J., Loveland, T.R., Kommareddy, A., Egorov, A.,  
744 Chini, L., Justice, C.O., Townshend, J.R.G., 2013. High-Resolution Global Maps of 21st-  
745 Century Forest Cover Change. *Science* 342, 850–853.  
746 <https://doi.org/10.1126/science.1244693>
- 747 29. IPBES, 2019. *Global Assessment Report on Biodiversity and Ecosystem Services of  
748 the Intergovernmental Science-Policy Platform on Biodiversity and Ecosystem Services*.  
749 IPBES secretariat, Bonn, Germany.
- 750 30. IPCC, Shukla, P.R., Skea, J., Calvo Buendia, E., Masson-Delmotte, V., Portner, H.-O.,  
751 Roberts, D.C., Zhai, P., Slade, R., Connors, S., Van Diemen, R., Ferrat, M., Haughey, E.,  
752 Luz, S., Neogi, S., Pathak, M., Petzold, J., Portugal Pereira, J., Vyas, P., Huntley, E.,  
753 Kissick, K., Belkacemi, M., Malley, J., 2019. *Climate Change and Land: an IPCC special  
754 report on climate change, desertification, land degradation, sustainable land management,  
755 food security, and greenhouse gas fluxes in terrestrial ecosystems*. IPCC.
- 756 31. Ju, J., Roy, D.P., 2008. The availability of cloud-free Landsat ETM+ data over the  
757 conterminous United States and globally. *Remote Sens. Environ.* 112, 1196–1211.  
758 <https://doi.org/10.1016/j.rse.2007.08.011>
- 759 32. Justice, C.O., Townshend, J.R.G., Vermote, E.F., Masuoka, E., Wolfe, R.E., Saleous,  
760 N., Roy, D.P., Morisette, J.T., 2002. An overview of MODIS Land data processing and  
761 product status. *Remote Sens. Environ.* 83, 3–15. [https://doi.org/10.1016/S0034-  
762 4257\(02\)00084-6](https://doi.org/10.1016/S0034-4257(02)00084-6)
- 763 33. Keenan, R.J., Reams, G.A., Achard, F., Freitas, J.V. [de, Grainger, A., Lindquist, E.,  
764 2015. Dynamics of global forest area: Results from the FAO Global Forest Resources  
765 Assessment 2015. *For. Ecol. Manag.* 352, 9–20.  
766 <https://doi.org/10.1016/j.foreco.2015.06.014>
- 767 34. Kendall, M.G., 1938. A New Measure of Rank Correlation. *Biometrika* 30, 81–93.  
768 <https://doi.org/10.1093/biomet/30.1-2.81>
- 769 35. Kirchner, M., Mitter, H., Schneider, U.A., Sommer, M., Falkner, K., Schmid, E., 2021.  
770 *Uncertainty concepts for integrated modelling - Review and application for identifying  
771 uncertainties and uncertainty propagation pathways*. *Environ. Model. Softw.* 135, 104905.

- 772 <https://doi.org/10.1016/j.envsoft.2020.104905>
- 773 36. Lehner, B., Verdin, K., Jarvis, A., 2008. New Global Hydrography Derived From  
774 Spaceborne Elevation Data. *Eos Trans. Am. Geophys. Union* 89, 93–94.  
775 <https://doi.org/10.1029/2008EO100001>
- 776 37. Lewińska, K., Frantz, D., Leser, U., Hostert, P., 2023. Usable Observations over  
777 Europe: Evaluation of Compositing Windows for Landsat and Sentinel-2 Time Series.  
778 Preprints. <https://doi.org/10.20944/preprints202308.2174.v2>
- 779 38. Li, D., Zhang, Z., 2023. MetaQA: Enhancing human-centered data search using  
780 Generative Pre-trained Transformer (GPT) language model and artificial intelligence. *PloS*  
781 *One* 18, e0293034. <https://doi.org/10.1371/journal.pone.0293034>
- 782 39. Liu, H., Gong, P., Wang, J., Wang, X., Ning, G., Xu, B., 2021. Production of global  
783 daily seamless data cubes and quantification of global land cover change from 1985 to 2020  
784 - iMap World 1.0. *Remote Sens. Environ.* 258, 112364.  
785 <https://doi.org/10.1016/j.rse.2021.112364>
- 786 40. Ma, X., Zhu, X., Xie, Q., Jin, J., Zhou, Y., Luo, Y., Liu, Y., Tian, J., Zhao, Y., 2022.  
787 Monitoring nature’s calendar from space: Emerging topics in land surface phenology and  
788 associated opportunities for science applications. *Glob. Change Biol.* 28, 7186–7204.  
789 <https://doi.org/10.1111/gcb.16436>
- 790 41. Mas, J.-F., Soares de Araújo, F., 2021. Assessing Landsat Images Availability and Its  
791 Effects on Phenological Metrics. *Forests* 12. <https://doi.org/10.3390/f12050574>
- 792 42. McNemar, Q., 1947. Note on the sampling error of the difference between correlated  
793 proportions or percentages. *Psychometrika* 12, 153–157.  
794 <https://doi.org/10.1007/bf02295996>
- 795 43. Meng, Z., Dong, J., Ellis, E.C., Metternicht, G., Qin, Y., Song, X.-P., Löfqvist, S.,  
796 Garrett, R.D., Jia, X., Xiao, X., 2023. Post-2020 biodiversity framework challenged by  
797 cropland expansion in protected areas. *Nat. Sustain.* [https://doi.org/10.1038/s41893-023-](https://doi.org/10.1038/s41893-023-01093-w)  
798 [01093-w](https://doi.org/10.1038/s41893-023-01093-w)
- 799 44. Michalak, A.M., Xia, J., Brdjanovic, D., Mbiyozo, A.-N., Sedlak, D., Pradeep, T., Lall,  
800 U., Rao, N., Gupta, J., 2023. The frontiers of water and sanitation. *Nat. Water* 1, 10–18.  
801 <https://doi.org/10.1038/s44221-022-00020-1>
- 802 45. Molder, E.B., Schenkein, S.F., McConnell, A.E., Benedict, K.K., Straub, C.L., 2022.  
803 Landsat Data Ecosystem Case Study: Actor Perceptions of the Use and Value of Landsat.  
804 *Front. Environ. Sci.* 9. <https://doi.org/10.3389/fenvs.2021.805174>
- 805 46. Mora, Wijaya, A., 2012. Capacity development in national forest monitoring:  
806 Experiences and progress for REDD+. *GOFC-GOLD, CIFOR, Bogor, Indonesia.*
- 807 47. Moyer, J.D., Hedden, S., 2020. Are we on the right path to achieve the sustainable  
808 development goals? *World Dev.* 127, 104749.  
809 <https://doi.org/10.1016/j.worlddev.2019.104749>
- 810 48. Mulligan, M., van Soesbergen, A., Sáenz, L., 2020. GOODD, a global dataset of more  
811 than 38,000 georeferenced dams. *Sci. Data* 7, 31. [https://doi.org/10.1038/s41597-020-0362-](https://doi.org/10.1038/s41597-020-0362-5)  
812 [5](https://doi.org/10.1038/s41597-020-0362-5)
- 813 49. Nackoney, J., Molinario, G., Potapov, P., Turubanova, S., Hansen, M.C., Furuichi, T.,  
814 2014. Impacts of civil conflict on primary forest habitat in northern Democratic Republic of  
815 the Congo, 1990–2010. *Biol. Conserv.* 170, 321–328.

- 816 <https://doi.org/10.1016/j.biocon.2013.12.033>
- 817 50. Olofsson, P., Foody, G.M., Herold, M., Stehman, S.V., Woodcock, C.E., Wulder, M.A.,  
818 2014. Good practices for estimating area and assessing accuracy of land change. *Remote*  
819 *Sens. Environ.* 148, 42–57. <https://doi.org/10.1016/j.rse.2014.02.015>
- 820 51. Pearson, T.R.H., Brown, S., Murray, L., Sidman, G., 2017. Greenhouse gas emissions  
821 from tropical forest degradation: an underestimated source. *Carbon Balance Manag.* 12, 3.  
822 <https://doi.org/10.1186/s13021-017-0072-2>
- 823 52. Pekel, J.-F., Cottam, A., Gorelick, N., Belward, A.S., 2016. High-resolution mapping  
824 of global surface water and its long-term changes. *Nature* 540, 418–422.  
825 <https://doi.org/10.1038/nature20584>
- 826 53. Perino, A., Pereira, H.M., Felipe-Lucia, M., Kim, H., Köhl, H.S., Marselle, M.R.,  
827 Meya, J.N., Meyer, C., Navarro, L.M., van Klink, R., Albert, G., Barratt, C.D., Bruelheide,  
828 H., Cao, Y., Chamoin, A., Darbi, M., Dornelas, M., Eisenhauer, N., Essl, F., Farwig, N.,  
829 Förster, J., Freyhof, J., Geschke, J., Gottschall, F., Guerra, C., Haase, P., Hickler, T., Jacob,  
830 U., Kastner, T., Korell, L., Kühn, I., Lehmann, G.U.C., Lenzner, B., Marques, A., Motivans  
831 Švara, E., Quintero, L.C., Pacheco, A., Popp, A., Rouet-Leduc, J., Schnabel, F., Siebert, J.,  
832 Staude, I.R., Trogisch, S., Švara, V., Svenning, J.-C., Pe'er, G., Raab, K., Rakosy, D.,  
833 Vandewalle, M., Werner, A.S., Wirth, C., Xu, H., Yu, D., Zinngrebe, Y., Bonn, A., 2022.  
834 Biodiversity post-2020: Closing the gap between global targets and national-level  
835 implementation. *Conserv. Lett.* 15, e12848. <https://doi.org/10.1111/conl.12848>
- 836 54. Potapov, P., Turubanova, S., Hansen, M.C., Tyukavina, A., Zalles, V., Khan, A., Song,  
837 X.-P., Pickens, A., Shen, Q., Cortez, J., 2022. Global maps of cropland extent and change  
838 show accelerated cropland expansion in the twenty-first century. *Nat. Food* 3, 19–28.  
839 <https://doi.org/10.1038/s43016-021-00429-z>
- 840 55. Prishchepov, A.V., Radeloff, V.C., Dubinin, M., Alcantara, C., 2012. The effect of  
841 Landsat ETM/ETM+ image acquisition dates on the detection of agricultural land  
842 abandonment in Eastern Europe. *Remote Sens. Environ.* 126, 195–209.  
843 <https://doi.org/10.1016/j.rse.2012.08.017>
- 844 56. Rasmussen, J., Madsen, H., Jensen, K.H., Refsgaard, J.C., 2016. Data assimilation in  
845 integrated hydrological modelling \hack\newline in the presence of observation bias.  
846 *Hydrol. Earth Syst. Sci.* 20, 2103–2118. <https://doi.org/10.5194/hess-20-2103-2016>
- 847 57. Rowland, J.A., Bland, L.M., James, S., Nicholson, E., 2021. A guide to representing  
848 variability and uncertainty in biodiversity indicators. *Conserv. Biol.* 35, 1669–1682.  
849 <https://doi.org/10.1111/cobi.13699>
- 850 58. Roy, D.P., Kovalskyy, V., Zhang, H.K., Vermote, E.F., Yan, L., Kumar, S.S., Egorov,  
851 A., 2016. Characterization of Landsat-7 to Landsat-8 reflective wavelength and normalized  
852 difference vegetation index continuity. *Remote Sens. Environ.* 185, 57–70.  
853 <https://doi.org/10.1016/j.rse.2015.12.024>
- 854 59. Sales, V.G., Strobl, E., Elliott, R.J.R., 2022. Cloud cover and its impact on Brazil's  
855 deforestation satellite monitoring program: Evidence from the cerrado biome of the  
856 Brazilian Legal Amazon. *Appl. Geogr.* 140, 102651.  
857 <https://doi.org/10.1016/j.apgeog.2022.102651>
- 858 60. Schmidt-Traub, G., Kroll, C., Teksoz, K., Durand-Delacre, D., Sachs, J.D., 2017.  
859 National baselines for the Sustainable Development Goals assessed in the SDG Index and